Storm-enhanced tidal sand transport - Hecate Strait, British Columbia, Canada

by

Carl L. Amos

Geological Survey of Canada
Atlantic Geocience Centre
P.O. Box 1006, Dartmouth, N.S.
CANADA

J. Timothy Judge

Martec Limited
1888 Brunswick St.
Dartmouth, N.S.
CANADA

and

J. Vaughn Barrie

Pacific Geoscience Centre
P.O. Box 6000
Sidney, B.C.
CANADA

OPEN FILE
DOSSIER PUBLIC
2604
GEOLOGICAL SURVEY
COMMISSION GEOLOGIQUE
OTTAWA

Background and purpose

Storm-enhanced tidal sand transport was hindcasted for a 1ø x 1ø geographic region approximately centred over Rose Spit; the northeastern tip of Graham Island in the Queen Charlotte Islands, northern British Columbia, Canada (Figure 1). The region is subject to intense storms that track northward through the region, often deepening explosively. General observations suggest that the waves and wind-driven currents associated with the passage of these storms play a major role in coastline erosion (known to be in excess of 20 m/year), in the longshore transport and sorting of shoreface sediments and in the bathymetry and morphology of shallow banks and tidal bedforms that characterize Hecate Strait (Figure 2).

The region is underlain by sediment sizes ranging from fine silts in the deep basins of Dixon Entrance in the north to coarse sand to the south (Figure 3). The majority of the coastal shoreface and adjacent Dogfish Bank is composed of fine sand moulded into shoreface-connected ridges, tidal ridges and shore-parallel ridges. Beyond the shoreface of Dogfish Bank is a region of medium sand that forms an arcuate band that encompasses Rose Spit. This Spit was considered to be an extension of the northeast point of Graham Island, fed by the longshore transport of sand that is derived by coastal erosion. The coastal cliffs, however, largely comprises fine sand not medium sand (Harper, 1980). So what is the origin of Rose Spit. Also, why does it not spill over into the deeper waters of Dixon Entrance given the dominance of southeasterly storm winds driving sediments to the north ? The purpose of this study was to examine the effects of storms on the transport of tidal sands in order to help explain these questions, and to provide information suitable for studies on alternatives for coastal protection.

The method

Predictions were made using the Geological Survey of Canada sediment transport numerical model - SEDTRANS. The structure of this model is shown in Figure 4. SEDTRANS integrates geological and hydrodynamical input data discritized and gridded on a 1 x 1 minute 2-D matrix. Geological data includes: bathymetry, sediment mean grain size and sediment sorting and density. These were derived from standard hydrographic charts and unpublished data held at Pacific Geoscience Centre. Hydrodynamical data include: tidal current speed and direction (we used the first 5 tidal constituents: M2, S2, N2, K2 and K1. These were derived from a predictive tidal model developed by Foreman and Walters (1990)); significant wave height, period and direction of propagation (These were derived from full spectral wave hindcasting undertaken by SeaConsult Marine Research Ltd. (1986), for the duration of the selected storm); storm-driven currents (these were derived from numerical predictions described by Hannah et al. (1991). The details of the model are described by Amos and Judge (1991). For this study we adopted the Grant and Madsen (1979) method for evaluation of combined flow bed stress, in association with the total sediment discharge algorithm of Engelund and Hansen (1967).

The storm

Predictions of sand transport were made for conditions of: (1) purely tidal sand transport; and (2) for a severe winter storm that occurred on 26 February, 1984; the most severe storm in the region in the decade of the 80's. The storm was the result of a large cyclone whose centre (of 882 mbars) was situated approximately 300 km west of the Queen Charlotte Islands in the north Pacific during its peak (1800 GMT). The pressure field of the storm created northerly kinematic winds over the entire study region that blew consistently for 24 hours. The resulting maximum significant wave height in Hecate Strait was 9.4 m. Although the magnitude of the storm was exceptional, the character of the storm was typical of the region.

Hydrodynamic processes

The physical environment of the Hecate Strait region has been described by Langford (1983). Tides in the region are mixed diurnal/semi-diurnal. Tidal range varies from 3 m in the south to 5 m in the north. The tidal wave propagates eastwards into Dixon Entrance and northwards through Hecate Strait. The two branches of the flood tide meet near Rose Spit approximately 1 hour into the flood stage, resulting in a complex flow pattern. The tidal flow (depth-averaged) in the region is strongly semi-diurnal with a moderate diurnal inequality. Figure 5 shows the tidal currents for the storm peak (1800 hours). Notice the strong ebb current over Rose Spit (circa 0.35 m/s) and the tidal divergence at the coast in the south of the region. The wave climate is illustrated in Figure 6. Here we see wave conditions during the storm peak. Notice the northward direction of propagation and the peak in wave height close to Rose Spit. Wind-driven currents (depth-averaged) are illustrated in Figure 7. The example shown is also for the storm peak. A maximum current speed of 0.75 m/s was predicted for the eastern extreme of the region where north-flowing tidal waters in Hecate Strait are accelerated through a narrow channel east of Rose Spit. In the shallower regions of Hecate Strait, wind-driven currents attain a speed of 0.45 m/s. To the north these currents decrease considerably. The flows are everywhere northward, except in MacIntyre Bay where a weak westward-directed flow is seen in the shallow water close to shore.

The total flow field for the peak (1800 GMT) of the 26 February, 1984 storm is shown in Figure 8. Notice the enhancement of flow in the vicinity of Rose Spit and the rapid decay and rotation parallel to isobaths in southern Dixon Entrance. Peak flows exceed 0.50 m/s on Rose Spit and maximize in the easternmost section of the region at 0.75 m/s at the peak of the storm.

Sediment transport and bed stability

In Figure 9, we present predicted net bed change brought about by the storm effects superimposed on tides for the day of the storm. Tidal flow causes very little change in bed elevation. Accretion is restricted to a narrow band along the northern flank of Rose Spit. Storm-induced bed changes were far more extensive and of greater magnitude than under tides alone. Erosion and accretion took place in unexpected spatial relationships. Furthermore, the majority of changes occurred during the peak of the storm. Erosion was greatest in a nearshore channel on central Dogfish Bank (0.001 mm/h), and was also prevalent on southern Dogfish Bank. The channel separating Graham Island from Rose Spit is also a site of intense erosion, particularly during the ebb tide. The submerged barrier (outer Dogfish Bank) was also subject to significant erosion. The regions of accretion were off the NE tip of Graham Island, on the flanks of the submerged barrier (eastern Dogfish Bank) and on the north flank of Rose Spit. The direction and magnitude of sand transport for tides alone is shown in three panels in Figure 10 (peak flood, storm peak and peak ebb). Notice that sand transport is low (circa 0.0001 kg/m/s) and restricted to Rose Spit and the channel at the tip of Graham Island.

Storm-induced sand transport is shown for 6 intervals for the duration of the storm in Figure 11. Notice there is significantly higher sand transport rates due to the storm, while a much greater portion of the seabed is mobilized. Peak sand transport rates are circa 0.05 kg/m/s. Virtually all of the region is under sand motion with a general movement of bed material from south to north in Hecate Strait. This transport comprises two transport cells; one centred on Rose Spit, the second over southern Dogfish Bank. Notice the strong convergence of sand transport at 0200 at the southern-most coastline along Hecate Strait. Also notice the westward movement of sand into MacIntyre Bay at the storm peak.

Interpretation and conclusions

The observed patterns of sand transport and accretion/erosion of the seabed fits geophysical, sedimentological and geomorphological observations made by the Pacific Geoscience Centre. Our results indicate that tidal sand transport is restricted to Rose Spit, and while significant, it has little effect on the long- term stability of the Spit. It is the superimposition of waves and wind-driven currents, generally associated with winter cyclones, that are responsible for the coastal and inner shelf sedimentary evolution. This through storm-enhanced sand transport. Sand transport is responsible for the winnowing of Southern Dogfish Bank and ablation of the submerged barrier island at its eastern edge. Thus we see coarse lag deposits in the southeast and an abundance of sand on northern Dogfish Bank.

The channel at the base of the shoreface is maintained by storm erosion as is the channel separating Graham Island from Rose Spit. The channel forms a barrier between shoreface sediments and their transport pathways and those of the inner shelf. There appears to be little transfer across this barrier.

Our results indicate that Rose Spit is not a spit in the true sense. It is more akin to a shelf-edge storm ridge. It has developed at a zone of sediment transport deceleration and rotation at the major change of slope along the north flank of Dogfish Bank. This zone of accretion we refer to as the "Hydraulic Fence" to sand transport, and is the same process that led to the formation of Sable Island, on the Scotian Shelf, Canada. The sand that is being added to Rose Spit is not derived from the shoreface of eastern Graham Island (due to the presence of an active channel at the base of the shoreface), but is a reworked product from southern Dogfish Bank. This is reflected in the grain size plot (Figure 3). Notice that the fine sand comprising the shoreface is not found on Rose Spit (which is medium and coarse in grain size). It is, however, evident in abundance in MacIntyre Bay, where a series of beach ridges have caused the coastline to prograde rapidly (Harper, 1980). Our results show that it is the north-flowing wind-driven current together with an ebbing tide that moves mobilized fine sand northward along the eastern coastline of Graham Island, through the nearshore channel, and thereafter westward into MacIntyre Bay.

The sand transport gyre on southern Dogfish Bank causes a convergence of sand along the south coast of Graham Island (see Figure 5). Here we find the presence of a wide beach bonded by a chaotic interfingering of weathered tree trunks. The beach has protected the cliff line from wave erosion, whereas to the north, where the beach is narrow, erosion is high. To what extend does the tree trunks induce beach formation and hence coastal protection ? Our results suggest that the beach (and associated tree trunks) is due to the nature of net storm-induced sand transport. The coastal protection would be afforded whether the tree were there or not. As a consequence the seeding of the coastline further north with tree trunks would have no influence on coastal stability given the rapid removal of beach sand during storms.

The model that we present herein appears to answer many basic questions regarding the origin and stability of surficial sediments along the coastline and inner shelf of northeastern Graham Island. While the model is for one storm only, it appears to fit geological interpretations based on geophysical and geomorphological evidence. A greater degree of certainty on results could be achieved by collection of calibration data on sediment transport. This is the focus of future efforts in the region.

References

Amos, C.L. and Judge, J.T. 1991. Sediment transport on the eastern Canadian continental shelf. Continental Shelf Research 11: 1037-1068.
Engelund, F. and Hansen, E. 1967. A monograph on sediment transport in alluvial streams. Teknisk Vorlag, Copenhagen, Denmark.
Foreman, M.C.C. and Walters, R.A. 1990. A finite-element tidal model for the southwest coast of Vancouver Island. Atmosphere-Ocean 28(3): 261-287.
Grant, W.D. and Madsen, O.S. 1979. Combined wave and current interaction with a rough bottom. Journal of Geophysical Research 84: 1797-1808.
Hannah, C. G. LeBland, P.H., Crawford, W.R. and Budgell, W.P. 1991. Wind-driven depth-averaged circulation in Queen Charlotte Sound and Hecate Strait. Atmosphere-Ocean 29(4): 712-736.
Harper, J.R. 1980. Coastal processes on Graham Island, Queen Charlotte Islands, British Columbia. Geological Survey of Canada Paper 80-1A: 13-18.
Langford, R.W. 1983. A preliminary environmental assessment of offshore hydrocarbon exploration and development. British Columbia Ministry of Environment Report: 334p.
SeaConsult Marine Research Ltd. 1986. On the impact of new observing sites on severe sea state warnings for the B.C. coast. Consultant Report prepared for Dept. Fisheries and Oceans, Sidney, B.C.

Acknowledgements are given to R. Courtney and the Digital Initiative Group, and to K. Edwardson for presenting this poster. This work was funded by PERD East Coast Project 63204.

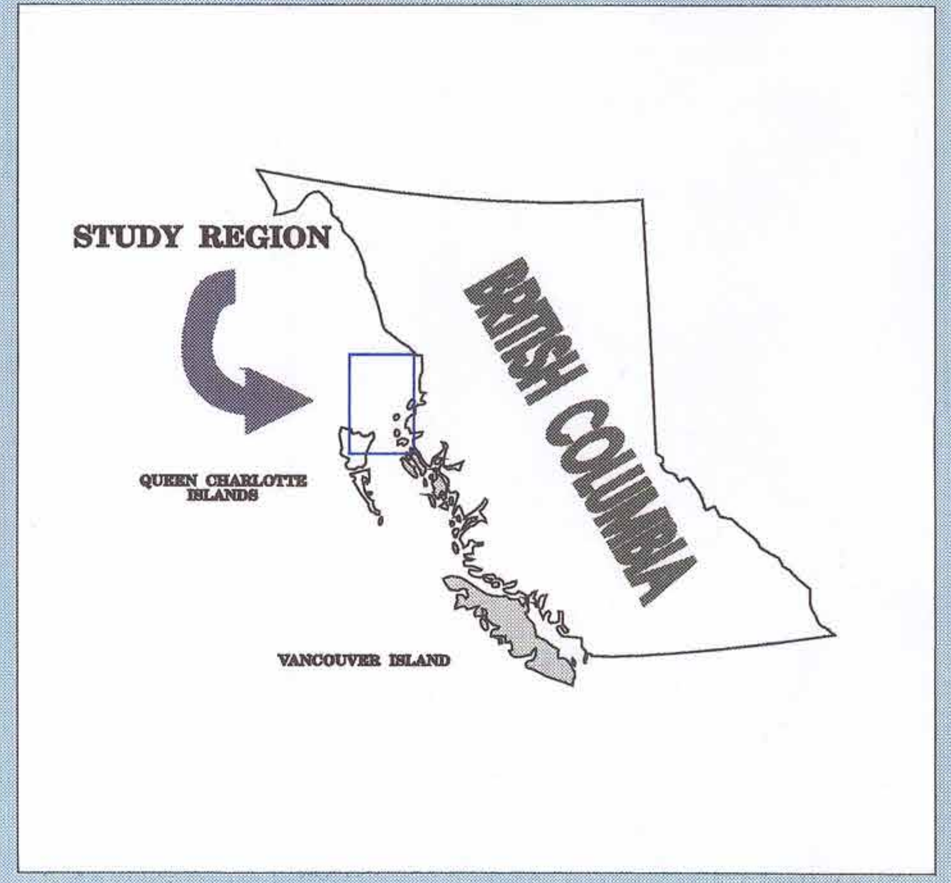

Figure 1 Location diagram of research region

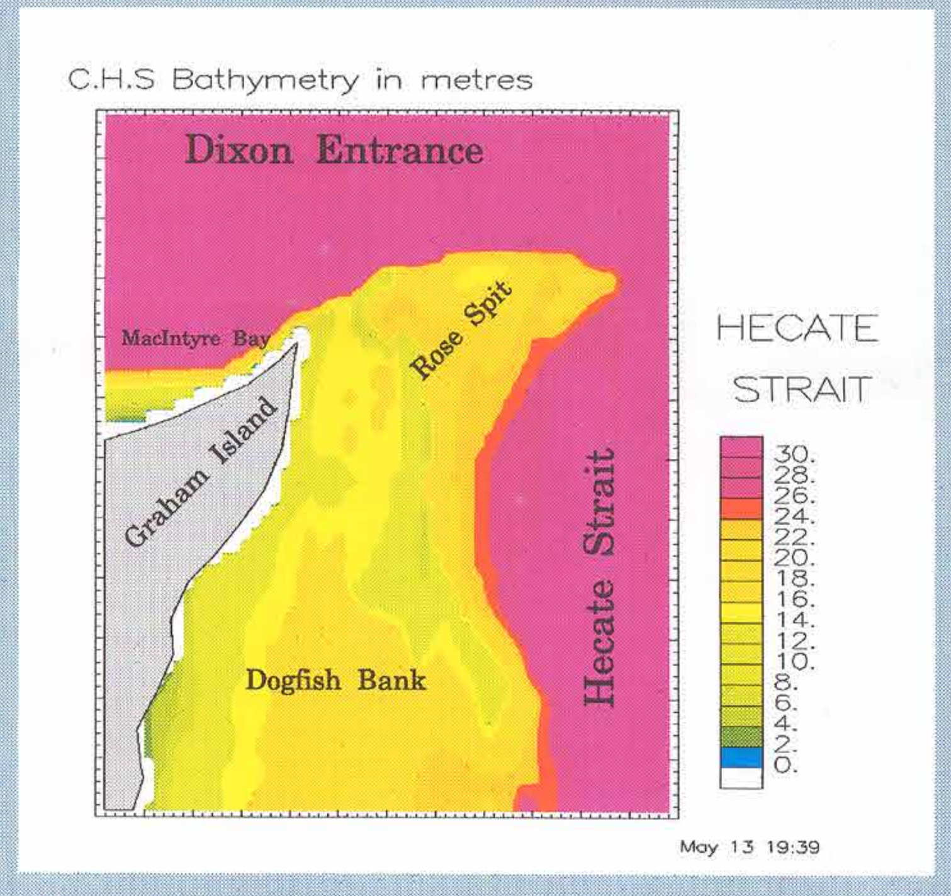

Figure 2. Detailed bathymetry of the Hecate Strait region.

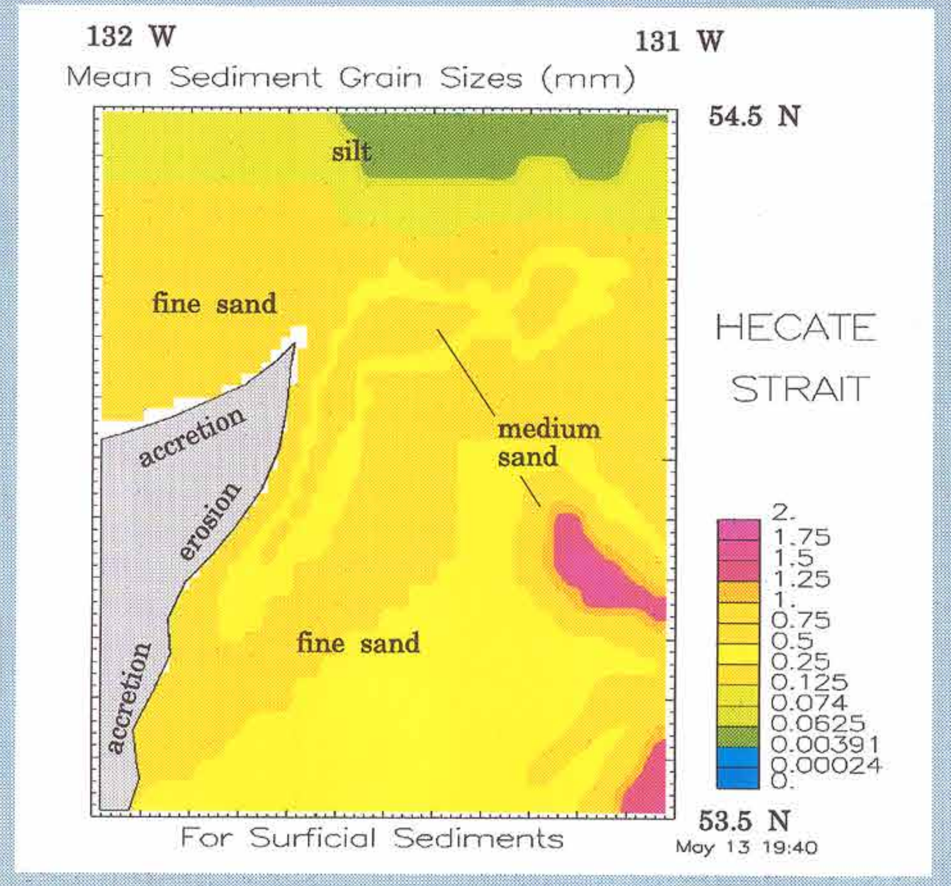

Figure 3. Mean grain size of bottom sediments.

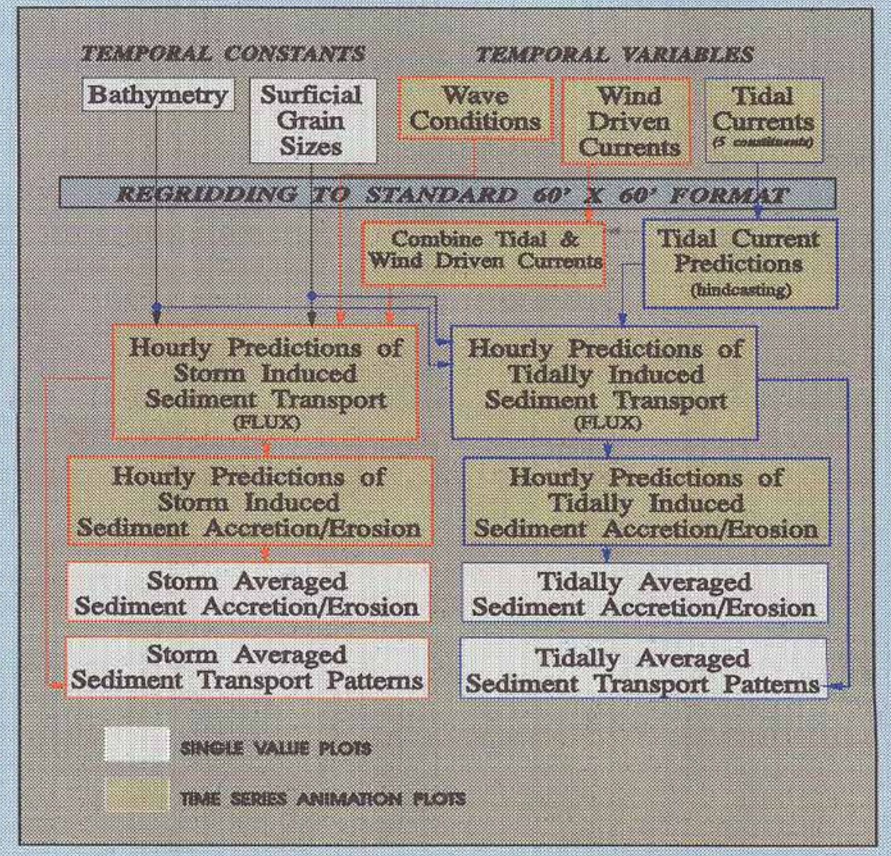
TEMPORAL CONSTANTS
TEMPORAL VARIABLES
Bathymetry
Surficial Grain Sizes
Wave Conditions
Wind Driven Currents
Tidal Currents
REGRIDDING TO STANDARD 60" X 60" FORMAT
Combine Tidal & Wind Driven Currents
Tidal Current Predictions
Hourly Predictions of Storm Induced Sediment Transport (FLUX)
Hourly Predictions of Tidally Induced Sediment Transport (FLUX)
Hourly Predictions of Storm Induced Sediment Accretion/Erosion
Hourly Predictions of Tidally Induced Sediment Accretion/Erosion
Storm Averaged Sediment Accretion/Erosion
Tidally Averaged Sediment Accretion/Erosion
Storm Averaged Sediment Transport Patterns
Tidally Averaged Sediment Transport Patterns
SINGLE VALUE PLOTS
TIME SERIES ANIMATION PLOTS

Figure 4. SEDTRANS flow chart.

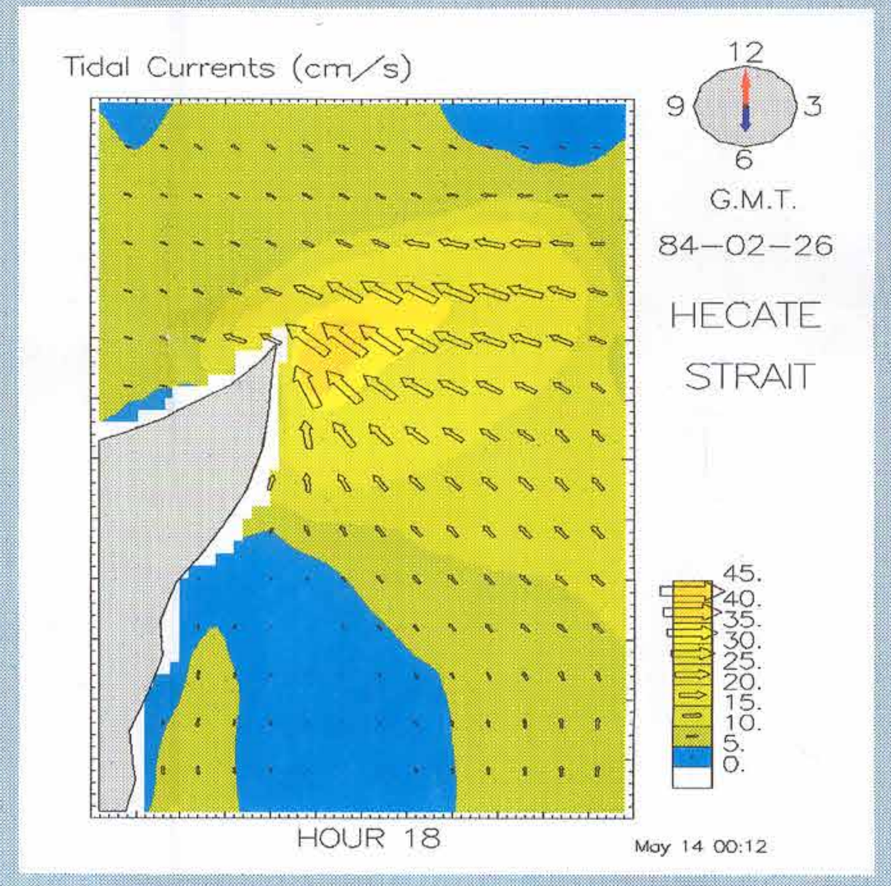

Figure 5. Tidal flow patterns at storm peak.

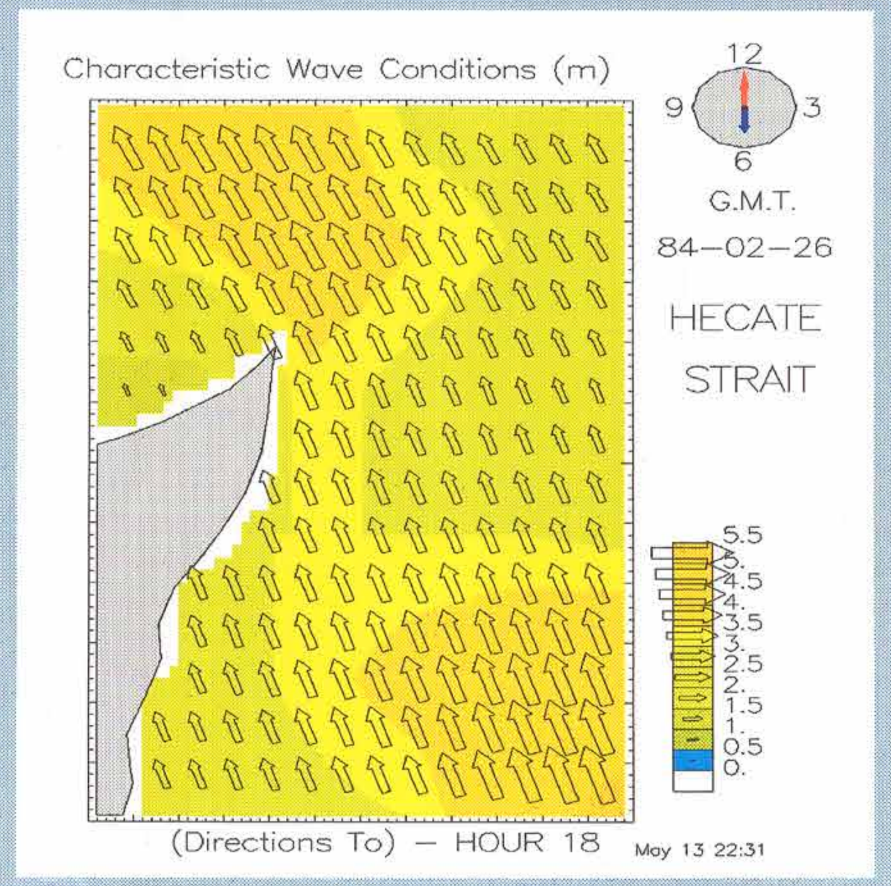

Figure 6. Wave climate at storm peak.

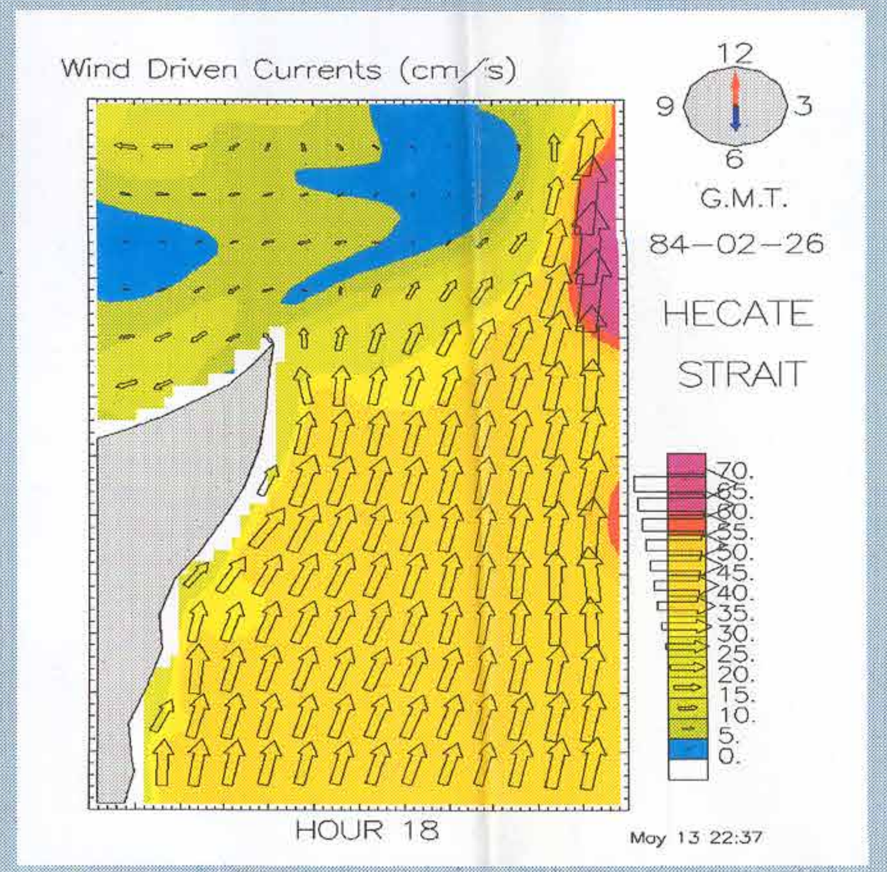

Figure 7. Wind-driven currents at storm peak.

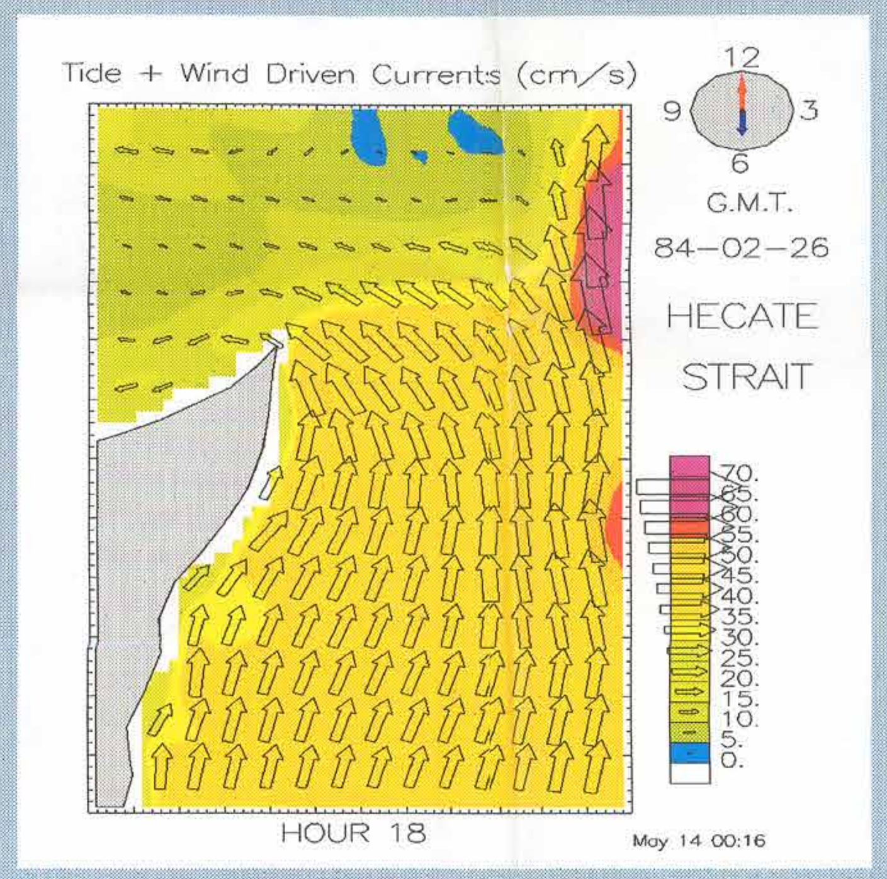

Figure 8. Total (storm + tides) current flow at storm peak.

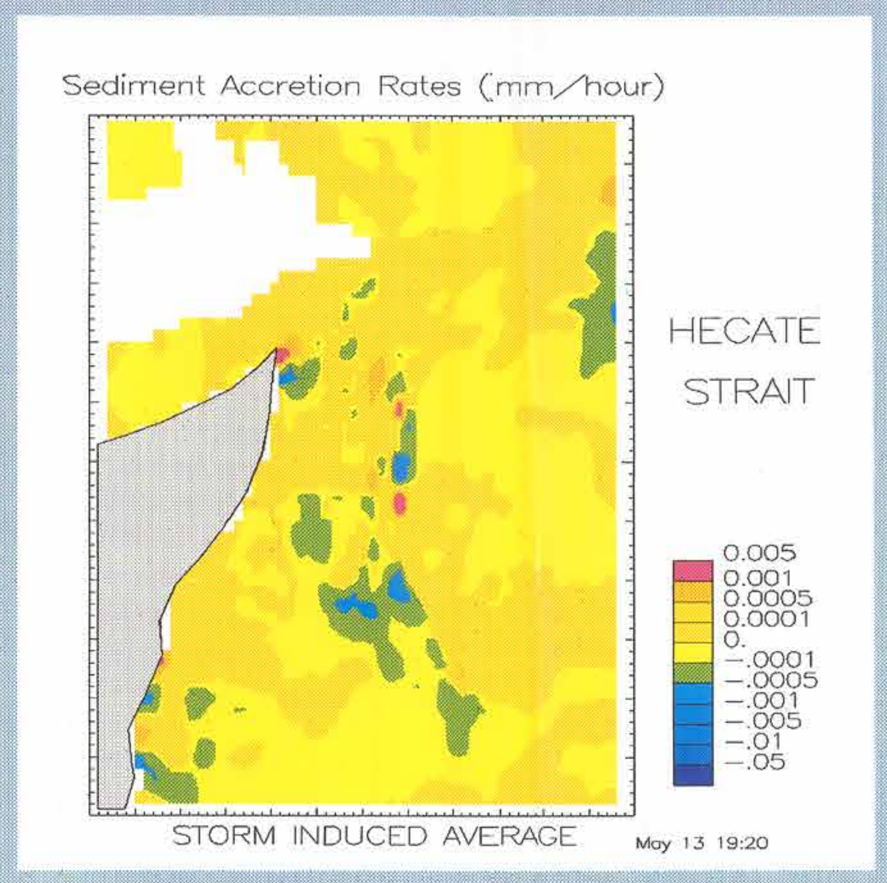

Figure 9. Predicted net sediment accretion/erosion.

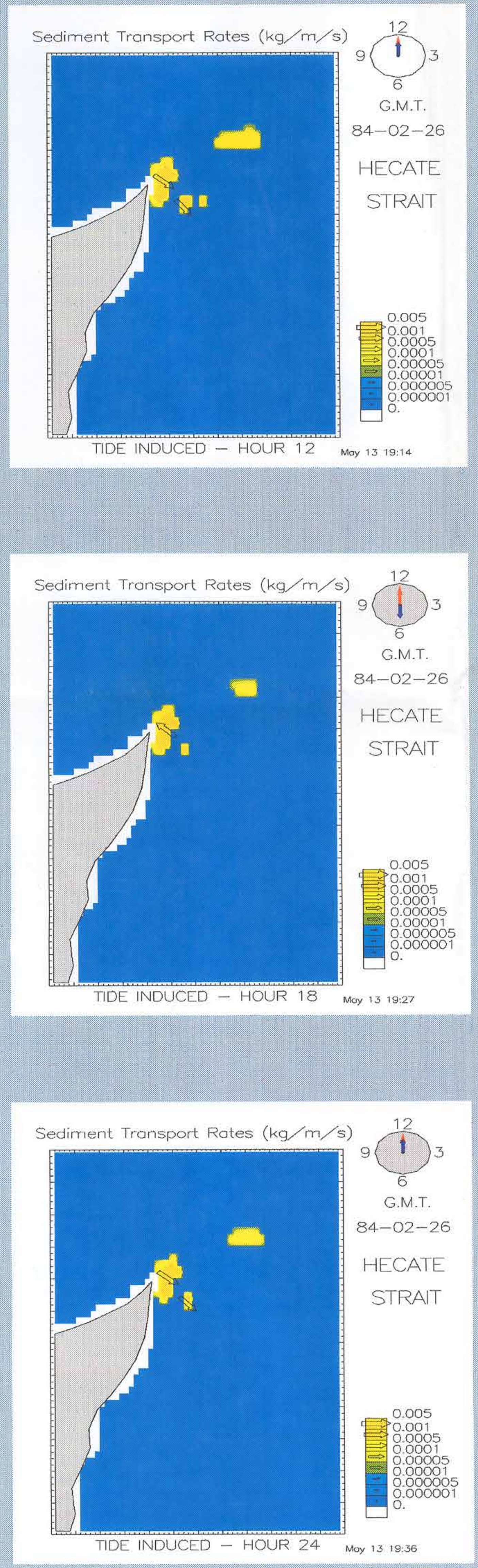

Figure 10. Predicted sediment transport patterns - tides only.

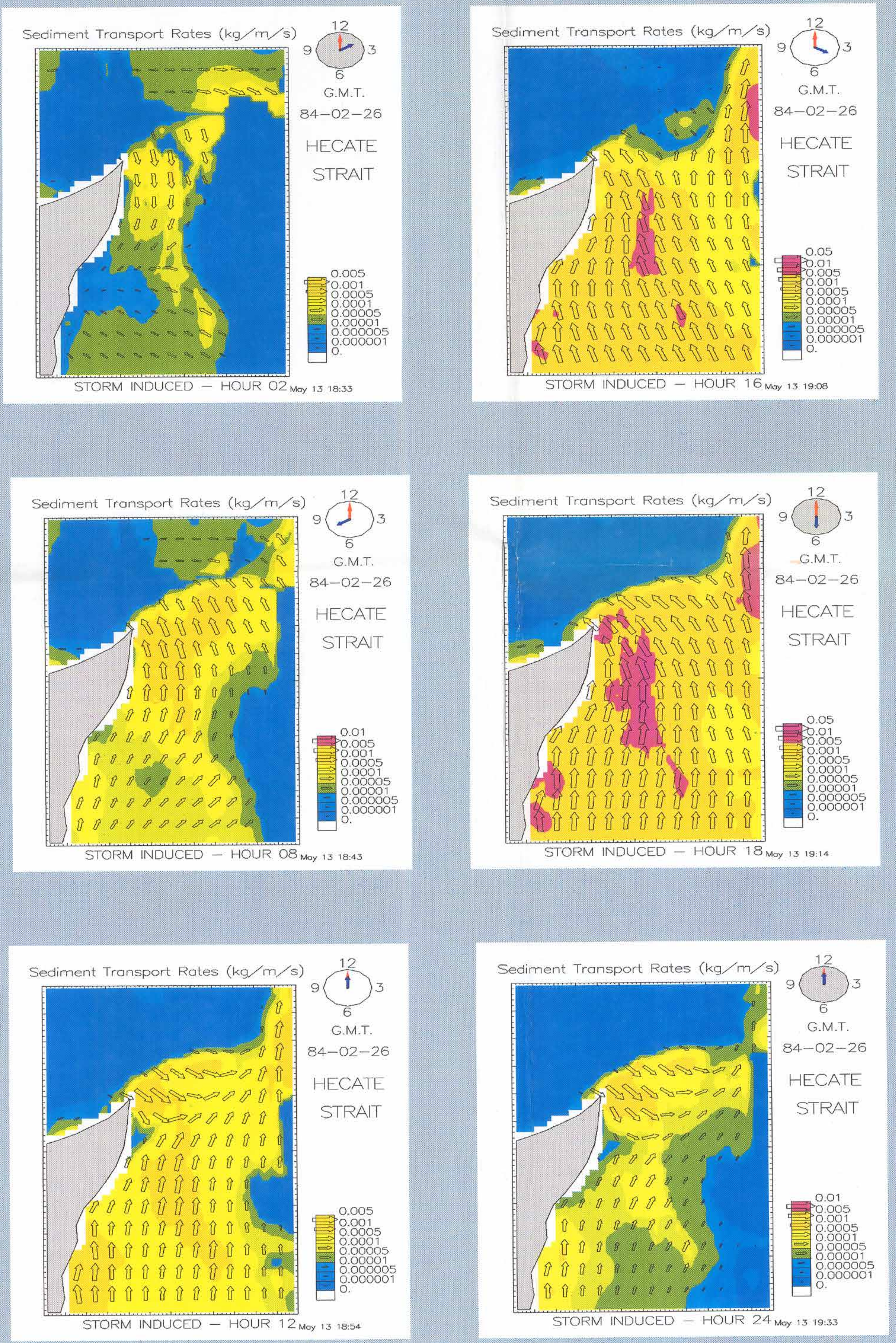

Figure 11. Predicted sediment transport patterns - tides + storm.

This document was produced by scanning the original publication.
Ce document est le produit d'une numérisation par balayage de la publication originale.